Quantitative Transmission Electron Microscopy in Substitutionally Disordered Alloys

Cyrille Barreteau and François Ducastelle
Office National d'Etudes et de Recherches Aérospatiales (ONERA), Direction des Matériaux (OM), B.P. 72, 92322 Châtillon Cedex, France
(Received 24 February 1995)

A simple channeling theory based on the atomic column approximation by Van Dyck *et al.* is used to relate the contrast of lattice images to the local concentrations in disordered alloys. The theory is shown to account for recent observations in pseudobinary semiconductor compounds and in metallic alloys.

PACS numbers: 61.14.Dc, 61.16.Bg, 68.35.–p

High resolution electron microscopy (HREM) is an invaluable tool to analyze crystalline structures, but several difficulties arise when trying to make it quantitative. Some of them are related to the experimental conditions: nature of the samples, optical aberrations, etc. At a more fundamental level, the strong interactions of electrons with matter prevents one from using the simple first order Born approximation (or kinematical theory) which is generally sufficient for treating neutron or x-ray diffraction [1]. Several different but equivalent theoretical and numerical methods have been devised to take into account multiple scattering of electrons. In the case of simple crystals, i.e., of elemental solids or of completely ordered compounds, Bloch theory can be used, and this basically reduces the problem to one similar to that treated in electron band theory. In practice, efficient numerical codes using so-called multislice techniques have been developed and are widely used [2,3].

Much less is known about disordered systems. We are dealing here with substitutionally disordered alloys on a fixed underlying lattice, and we would like to know whether lattice images can provide at least semiquantitative information on the concentration of atomic columns. Except for very thin samples, the relation between the electronic density at the exit plane and the atomic potentials is not simple, but several attempts have been made to define experimental conditions for which it can be quasilinear. There are several methods for doing that. The first one is to simulate lattice images with the available multislice codes, using sufficiently large boxes or real space techniques, but then physical insight is almost completely missing. Another approach recently put forward by Ourmazd *et al.* [4] is to make use of pattern recognition procedures to analyze the images. By correlating the input and the output for several model systems it is possible to define the conditions for which reliable interpolation procedures can be used. This is a quite useful tool but, of course, it does not provide explanations for the observed behaviors. Finally, other image processing algorithms based on a simple perturbative treatment of disorder have also been discussed by De Jong and Van Dyck [5].

Before applying to HREM the efficient techniques which have been developed for calculating the electronic structure of disordered systems [6], simple models are obviously desirable, and the basis for them is available. It has been observed for a fairly long time now that when the incident electron beam is parallel to well separated atomic columns channeling along these columns occurs up to about a few tens of nanometers. The equations describing electron propagation can then be simplified considerably, which allows one to obtain very attractive semiquantitative descriptions. This theory called the atomic column approximation (ACA) has been developed with success by Van Dyck *et al.* [7] but has not been applied so much yet to the treatment of disordered alloys (see, however, Ref. [8]).

In this Letter we present such a treatment. Using the simplest formulation, the wave function at the bottom of an atomic column containing different types of atoms is shown to contain a phase factor directly related to the numbers of these atoms in the column and to their scattering strengths. Fluctuations of local atomic concentrations therefore induce fluctuations of the phase whose magnitude increases when the thickness and the atomic contrast increase. This has simple and important consequences for the analysis of lattice images, even if the additional effect of the aberrations due to the HREM imaging process is not considered here. Some applications to semiconductor and metallic alloys will be presented.

We first recall the required formalism. For high energy electrons, backscattering can be neglected and the relevant Schrödinger equation is conveniently written as a two-dimensional evolution equation where the thickness z plays the part of time [9],

$$i\,\partial/\partial z|\psi_z\rangle = \mathcal{H}|\psi_z\rangle, \qquad \mathcal{H} = (H - \boldsymbol{q}_i^2)/2k_i^z . \quad (1)$$

$\boldsymbol{q}_i$ and k_i^z are the transverse and longitudinal components of the wave vector $\boldsymbol{k}_i$ of the incoming electron; $H = -\Delta_{\boldsymbol{\rho}} + V$ where $\Delta_{\boldsymbol{\rho}}$ is the two-dimensional kinetic energy $\partial^2/\partial x^2 + \partial^2/\partial y^2$ and $V(\boldsymbol{\rho}, z)$ is the potential energy at point $\boldsymbol{r} = (\boldsymbol{\rho}, z)$. In principle it depends on "time" z, but in many cases it can reasonably be replaced by its projection along the z axis. At least this can be done if the projection concerns a thin slab of thickness d. Typically for all the simple structures considered in the following

 0031-9007/95/75(2)/284(4)$06.00 © 1995 The American Physical Society

(fcc-based alloys, zinc-blende structure) d will be taken to be equal to the size of the unit cell along the z axis, i.e., between 0.2 and 0.6 nm. $V(\boldsymbol{\rho}, z)$ is then replaced by $V(\boldsymbol{\rho}) = \int_0^d V(\boldsymbol{\rho}, z)\, dz/d$. The formal integration of the evolution equation for the slab is then obvious,

$$|\psi_z\rangle = U(z,0)|\psi_0\rangle, \qquad U(z,0) = \exp(-i\,\mathcal{H} z). \quad (2)$$

In HREM the initial state is a plane wave $|\psi_0\rangle = |\boldsymbol{q}_i\rangle$, and usually the incident beam is taken along a high symmetry axis (symmetric Laue conditions, $\boldsymbol{q}_i = 0$). If the projection operation is repeated in successive slices $(0, z_1), (z_1, z_2), \ldots, (z_{p-1}, z_p)$, the full evolution operator $U(z_p, 0)$ is equal to $U(z_p, z_{p-1}), \ldots, U(z_1, 0)$ where the corresponding two-dimensional potentials V_p and Hamiltonians H_p are used in each slice. Now let $|\alpha\rangle$ and ε_α be the eigenstates and eigenvalues of the Hamiltonian H, $H|\alpha\rangle = \varepsilon_\alpha|\alpha\rangle$ so that $\mathcal{H}|\alpha\rangle = \gamma_\alpha|\alpha\rangle$ with $\gamma_\alpha = [\varepsilon_\alpha - (\boldsymbol{q}_i)^2]/2k_i^z$. Within a slice the evolution operator can be written $U(z,0) = \sum_\alpha |\alpha\rangle \exp(-i\,\gamma_\alpha z)\langle\alpha|$ and the wave function is given by $|\psi_z\rangle = \sum_\alpha C_\alpha \times \exp(-i\gamma_\alpha z)\,|\alpha\rangle$, where $C_\alpha = \langle\alpha|0\rangle$ is the excitation coefficient of state $|\alpha\rangle$.

In the case of periodic structures, the Bloch theorem applies and we can calculate two-dimensional band structures [10]. In all cases, whatever the atoms, whatever the acceleration voltage, it is found that there is one very localized bound $1s$ state per column [7,11]. In symmetric Laue conditions, the state is strongly excited and the only other excited states have energies close to zero. For well separated atomic columns the localized states do not overlap so that the above picture is also valid for a slice of disordered alloy. It is then convenient to separate out these states from the others. Therefore let P_c be the projector on the $1s$ core states, $P_c = \sum_n |n\rangle\langle n|$, where the two-dimensional states of columns n, $|n\rangle$, are assumed to form a set of orthonormalized states. Then

$$U(z,0) = \sum_n e^{-i\,\gamma_n z}|n\rangle\langle n| + (1 - P_c)e^{-i\mathcal{H}z}, \quad (3)$$

where γ_n is the $1s$ bound state energy of column n. Now, since the other excited states have energy close to zero, we can replace the second exponential by unity provided the thickness z is not too large. Finally, using the orthogonality relationship $\langle n|m\rangle = \delta_{n,m}$, the evolution operator corresponding to the ACA can be written as

$$U^{\mathrm{ACA}} = \prod_n U_n = 1 + \sum_n (U_n - 1),$$
$$U_n = 1 + (e^{-i\gamma_n z} - 1)|n\rangle\langle n|. \quad (4)$$

Within this approximation all column operators U_n commute, all columns are independent, and channeling is perfect. This simple approximation reproduces fairly well the dynamical effects as calculated from full calculations. This is illustrated in Fig. 1 in the case of the Ni_3Al ordered compound. In this example the atomic columns

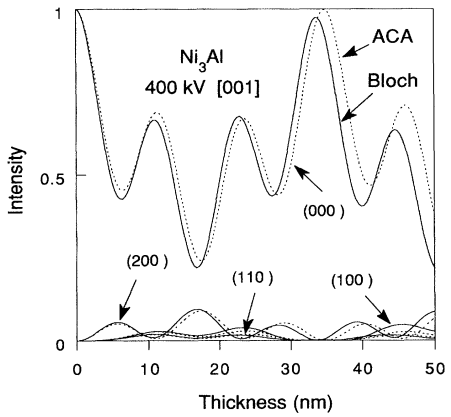

FIG. 1. Variation of intensity with sample thickness for the (000) transmitted beam and for the (100), (110), and (200) diffracted beams in Ni_3Al. The zone axis is [001] and the accelerating voltage is equal to 400 kV. Full line: Bloch calculation using 400 plane waves; dotted line: ACA result.

are pure Ni or pure Al columns so that projecting the potential over the unit cell is equivalent to projecting over the whole crystal. In this calculation, the previous formula has been slightly modified by introducing a small constant shift of the energy of the bound states, which is easy to justify; more details will be given elsewhere. It is clear that the ACA is very good up to at least 30 nm. The ACA would not be so good with heavier elements for which other bound or quasibound states can appear.

Let us now treat disordered alloys. To do that, we make repeated use of Eq. (4) for the successive slices labeled by p. In general the part of column n contained in slice p denoted (n, p) contains a single atomic site, which will be assumed in the following, but this is not a necessity. The ACA evolution operator U_n corresponding to column n is then written as

$$U_n = U_n^N \cdots U_n^p \cdots U_n^1,$$
$$U_n^p = 1 + (e^{-i\,\gamma_{n,p}\,d} - 1)\,|n,p\rangle\langle n,p|, \quad (5)$$

where $|n,p\rangle$ is the localized state of the atom at site (n,p) and N is the number of slices. The full ACA evolution operator is given by $U^{\mathrm{ACA}} = \prod_n U_n = 1 + \sum_n (U_n - 1)$.

The localized states are different for the A and B atoms of a binary alloy A_cB_{1-c}, so in principle the order of the operators in the above formula does matter, and the wave function at the exit plane of the sample depends not only on the numbers $N_n^{A(B)}$ ($N_n^A + N_n^B = N$) of A (B) atoms, but also on the detailed arrangement of the atoms in the column; this leads to the so-called top-bottom effect [8,12]. In fact, a first simple approximation is to take into account the difference between the energy levels $\gamma_{n,p} = \gamma^A$ or γ^B, depending on the occupation of site (n,p), while neglecting the difference between the $1s$ wave functions. This is the approximation currently made in the theory of disordered alloys treated within the tight-binding approximation. This approximation is certainly

reasonable when $|\gamma^A - \gamma^B|$ is not too large compared to the mean value $\langle\gamma\rangle = c\gamma^A + (1-c)\gamma^B$. Assuming then a single mean localized state, we can drop the label p and use a single state $|n\rangle$ per column, and finally in this simplified ACA scheme (SACA), the evolution operator is given by

$$U_n^{\mathrm{SACA}} = 1 + (e^{-i(N_n^A\gamma^A + N_n^B\gamma^B)d} - 1)\,|n\rangle\langle n|\,. \quad (6)$$

Note that this approximation is *not* equivalent to the projected potential approximation: the mean $1s$ level $\langle\gamma\rangle$ is not identical to the $1s$ level of the mean potential; in practice they are not so different. We have therefore shown that the validity of the ACA implies to some extent the validity of the projected potential approximation for disordered alloys. Top-bottom effects are not expected to be so important except for heavy elements and large thicknesses. This is actually what is observed in some recent numerical calculations [8,12].

Now let θ_n denote the phase factor in Eq. (6) and let $\psi_n^{1s}(\boldsymbol{\rho}) = \langle\boldsymbol{\rho}|n\rangle$ be the $1s$ wave function centered on column n. The electronic density, or intensity, at the exit plane $I(\boldsymbol{\rho}, z)$ is given by $|\langle\boldsymbol{\rho}|U(z,0)|\boldsymbol{q}=0\rangle|^2$. Neglecting the overlap between different $1s$ wave functions, the intensity at the exit of column n is given by

$$I_n(\boldsymbol{\rho}, z) = 1 - 2C^{1s}\psi_n^{1s}(\boldsymbol{\rho}) \times [1 - C^{1s}\psi_n^{1s}(\boldsymbol{\rho})](1 - \cos\theta_n)\,, \quad (7)$$

where the excitation coefficient C^{1s} is equal to $\int d\boldsymbol{\rho}\,\psi_n^{1s}(\boldsymbol{\rho})$ and the phase θ_n can be written

$$\theta_n = (N_n^A\gamma^A + N_n^B\gamma^B)\,d = [c_n\gamma^A + (1-c_n)\gamma^B]z\,, \quad (8)$$

where c_n is the concentration in A atoms of column n, $c_n = N_n^A/N$. It can easily be shown that the factor in front of $1 - \cos\theta_n$ is negative at the center of the column so that maximum contrast is obtained when $\cos\theta_n = -1$.

Consider now a completely disordered alloy. The probability distribution of the number of A atoms in the columns is binomial, with variance $Nc(1-c)$, and so is the probability distribution of θ considered as a stochastic variable whose possible values are the θ_n. Its mean value is $\langle\theta\rangle = \langle\gamma\rangle z$ and its variance σ^2 is given by

$$\sigma^2 = Nc(1-c)\,(\gamma^A - \gamma^B)^2 d^2, \quad (9)$$

but we are interested in the probability distribution of $\cos\theta_n$, which makes a big difference. Actually when N is very large the distribution of θ becomes Gaussian, but its width σ is much larger than 2π so that the distribution of $\theta(\mathrm{mod}2\pi)$ tends to a constant, independent of the concentration, the distribution of $u = \cos\theta$ tending to $1/\pi\sqrt{1-u^2}$. There is no central limit for the intensity distribution. When σ is small, the distribution is a genuine discrete distribution, but the phase is small anyway, and we recover the weak phase object limit; the intensity contrast is proportional to θ_n^2.

The interesting situation occurs in the intermediate case, when σ is large enough for the Gaussian limit to be valid while being small compared to 2π. In such a situation we expect a distribution of $\cos\theta$ centered on its mean, $\langle\cos\theta\rangle = \cos\langle\theta\rangle\exp(-\sigma^2/2)$. Its variance, i.e., its second order cumulant, is given by

$$\langle\cos^2\theta\rangle_c = (1 - e^{-\sigma^2})[(1 - e^{-\sigma^2})/2 + e^{-\sigma^2}\sin^2\langle\theta\rangle] \simeq \sigma^2\sin^2\langle\theta\rangle \quad \text{when} \quad \sigma \to 0\,. \quad (10)$$

The third centered moment is of order σ^4 when σ is small and has the opposite sign of $\cos\langle\theta\rangle$. The distribution is evidently particular and asymmetric when $\sin\langle\theta\rangle = 0$, i.e., when the contrast is minimum or maximum, $\cos\langle\theta\rangle = \pm 1$ (see Fig. 2).

From this discussion it is clear that the intensity can be related to the mean concentration c when σ is small compared to unity, which means that the thickness as well as the "atomic" contrast $|\gamma^A - \gamma^B|$ should not be too large. The atomic contrast depends on the electronic form factors, on the lattice parameter, and on the accelerating voltage, but the last dependence is weak. Note also that the situation where the contrast is the largest, $\sin\langle\theta\rangle = 0$, is more favorable. The mean deviation σ is therefore a very nice measure of the importance of dynamical effects. More precisely, $\sigma|\sin\theta|$ measures the fluctuations of the intensity induced by the concentration fluctuations. When it is of the order of unity we expect the intensity to display spots of almost random intensity, with a preference for the less and more intense spots. For smaller values of σ we expect on the contrary a fairly uniform intensity reflecting the value of the mean concentration.

We can now treat the case of an interface between regions of different concentrations. Assume, for example, a planar interface such that a mean concentration c_n can be defined for each plane parallel to the interface. The relevant variance as well as $\langle\theta\rangle$ now depends on n. If σ_n^2 is too large, the previous discussion shows that the interface would hardly be visible because of the very low signal-to-noise ratio. If σ_n is small enough, the electronic den-

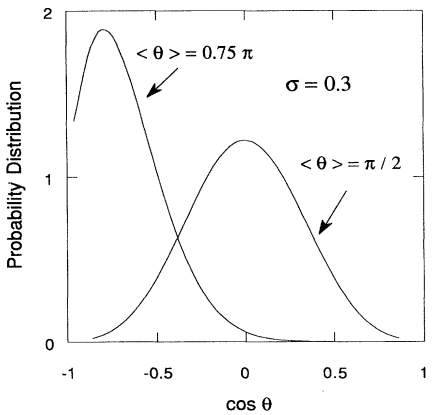

FIG. 2. Probability distribution of $\cos\theta$ for $\langle\theta\rangle = \pi/2$ and $\langle\theta\rangle = 0.75\pi$, assuming a Gaussian distribution for θ, with $\sigma = 0.3$.

sity will reflect the local concentration through $\cos\langle\theta_n\rangle = \cos[c_n\gamma^A + (1 - c_n)\gamma^B]z$. This is a nonlinear relationship except when the variation of $c_n(\gamma^A - \gamma^B)z$ along the concentration profile is small compared to 2π.

Let us apply this analysis to some cases treated recently. Consider first the concentration gradient in $Al_cGa_{1-c}As$ [4]. Using simple two-dimensional atomic calculations for an accelerating voltage of 400 kV we obtain $\gamma^{Al} = -0.12\ nm^{-1}$ and $\gamma^{Ga} = -0.30\ nm^{-1}$. Taking the thickness $z = 17$ nm ($N \simeq 30$) yields $\sigma = 0.56\sqrt{c(1 - c)} \leq 0.28 \simeq 2\pi/20$. We are therefore in a very favorable situation, and the intensity should respond reliably to concentration variations. In the case studied by Ourmazd *et al.* the concentration varies between 0 and 0.4. This corresponds to phases θ equal to 5 and 3.8, respectively, and the response should be quasilinear, as found by these authors. This is also in agreement with the detailed analysis of these semiconductor alloys by De Jong and Van Dyck [5]. Their theoretical analysis is based on a perturbation treatment of the concentration fluctuations which reproduces perfectly our general formulation in this limit.

We now consider a more problematic case where some heavy gold atoms replace aluminum atoms in Ni_3Al. The atomic contrast is large; at 400 kV we find $\gamma^{Al} = -0.24\ nm^{-1}$, $\gamma^{Au} = -2.10\ nm^{-1}$. For a thickness of 17 nm we find $\sigma = 4.55\sqrt{c(1 - c)} \leq 2.27 \simeq \pi$. This phase fluctuation corresponds to a concentration fluctuation of gold atoms $\sqrt{c(1 - c)/N}$ about 7%. Fairly small concentration fluctuations will therefore completely reverse the contrast. Such effects have been observed recently [13]. Actually for such heavy atoms and such a thickness the SACA scheme and the ACA itself begin to breakdown, but preliminary calculations clearly indicate that the previous picture is not strongly altered.

The present theory provides very simple criteria to understand many experimental results in disordered alloys. Several extensions and other applications can be considered and will be presented elsewhere. Deviations from the SACA can be dealt with. This does matter when one is interested in the analysis of diffracted beams and of diffuse scattering. Finally the influence of the transfer of the microscope must be taken into account to develop a full quantitative theory.

The assistance of A. Finel for the numerical calculations as well as many fruitful discussions with D. Gratias and A. Loiseau are gratefully acknowledged.

[1] J. M. Cowley, *Diffraction Physics* (North-Holland, Amsterdam, 1981), 2nd ed.
[2] P. A. Stadelmann, Ultramicroscopy **21**, 131 (1987).
[3] D. Van Dyck and W. Coene, Ultramicroscopy **15**, 29 (1984); W. Coene and D. Van Dyck, Ultramicroscopy **15**, 41 (1984); **15**, 287 (1984).
[4] A. Ourmazd, F. H. Baumann, M. Bode, and Y. Kim, Ultramicroscopy **34**, 237 (1990); P. Schwander, C. Kisielowski, M. Seibt, F. H. Baumann, Y. Kim, and A. Ourmazd, Phys. Rev. Lett. **71**, 4150 (1993).
[5] A. F. De Jong and D. Van Dyck, Ultramicroscopy **33**, 269 (1990).
[6] For a review, see, e.g., F. Ducastelle, *Order and Phase Stability in Alloys* (North-Holland, Amsterdam, 1991).
[7] D. Van Dyck, J. Danckaert, W. Coene, E. Selderlaghs, D. Broddin, J. Van Landuyt, and S. Amelinckx, in *Computer Simulation of Electron Microscope Diffraction and Images,* edited by W. Krakow and M. O'Keefe (The Minerals, Metals and Materials Society, Warrendale, PA, 1989), p. 107; see also S. Amelinckx and D. Van Dyck, in *Electron Diffraction Techniques,* edited by J. M. Cowley (IUCr-Oxford University Press, Oxford, 1993), Vol. 2, p. 1.
[8] P. De Meulenaere, D. Van Dyck, G. Van Tendeloo, and J. Van Landuyt, "Dynamical Electron Diffraction in Substitutionally Disordered Column Structures" (to be published).
[9] D. Van Dyck, J. Microsc. **119**, 142 (1980); D. Gratias and R. Portier, Acta Crystallogr., Sect. A **39**, 576 (1983).
[10] C. Barreteau and F. Ducastelle, Ultramicroscopy **57**, 11 (1995).
[11] K. Kambe, G. Lempfuhl, and F. Fujimoto, Z. Naturforsch. **29A**, 1034 (1974).
[12] W. Coene, D. Van Dyck, J. Van Landuyt, and S. Amelinckx, Philos. Mag. B **56**, 415 (1987).
[13] J. M. Pénisson, Ultramicroscopy **51**, 264 (1993); interfaces in Ni-based superalloys have also been studied: J. M. Pénisson, M. Bode, F. H. Baumann, and A. Ourmazd, Philos. Mag. Lett. **64**, 269 (1991); for similar studies for antiphase boundaries in Cu_3Pd, see also A. Loiseau, J. M. Pénisson, and J. Planès, J. Interface Sci. (to be published).